

# FINITE ELEMENTS CALCULATIONS OF THE LATTICE AND RING ACCEPTANCE OF THE HEIDELBERG CSR

H. Fadil\*, M. Grieser, R. von Hahn and A. Wolf, MPI-K Heidelberg, Germany

## Abstract

A new Cryogenic Storage Ring (CSR) is currently being designed at MPI-K in Heidelberg. This electrostatic ring, which will store ions in the 20 – 300 keV energy range (E/Q), has a total circumference of 35.2 m and a straight section length of 2.8 m. The ring design was at first carried out with the optics code MAD in the first order approximation. Further investigation of the optics was performed with the finite elements electrostatic code TOSCA. The fields of the individual elements of the CSR (deflectors and quadrupoles) were calculated and then a model of the entire ring was simulated with successful storage (tracking) of 20 keV protons for many turns. The lattice parameters thus obtained were compared with the MAD results and show good agreement. The dynamic ring acceptance was also calculated for the standard operating point.

## INTRODUCTION

Electrostatic storage rings have become invaluable tools for molecular and atomic physics research recently. In the low energy regime, electrostatic deflection and focusing elements are more efficient than magnetic ones. In magnetic storage rings, the mass of the particles which can be stored is limited by the magnetic rigidity, whereas for an electrostatic ring the rigidity depends only on the particle charge and energy. Presently, there are three electrostatic storage rings in operation [1,2,3]. The first two rings operate at room temperature while the last one was designed for operation at liquid nitrogen temperature. At the Max-Planck Institut für Kernphysik a new electrostatic storage ring CSR, operating at cryogenic temperatures below 4 K is under construction [4]. By the use of electrostatic deflectors and focusing elements, ions with kinetic energies in the range 20 – 300 keV can be stored without any mass limitation. An electron cooler, based on photo-cathode technology developed for the TSR [5], will be used to cool the ions and to study electron ion interactions.

## THE LATTICE

The ring lattice shown in Figure 1 consists of electrostatic cylindrical deflectors and quadrupole doublets. The 90° bend at each corner is separated into two 6° deflectors with a bending radius of 2 m and two 39° deflectors with a radius of 1 m. The main advantages of this layout is the ease of single turn injection, since only a fast switching (comparable to the revolution time) of the 6° deflector is

necessary to inject the beam. Also the merging of neutral or laser beams with the rotating ions can be realised along a straight section through the gap between the two types of deflectors. In addition, it is important to be able to detect various neutral and charged reaction fragments, which is possible with this arrangement.

To focus the beam, two quadrupole doublets placed before

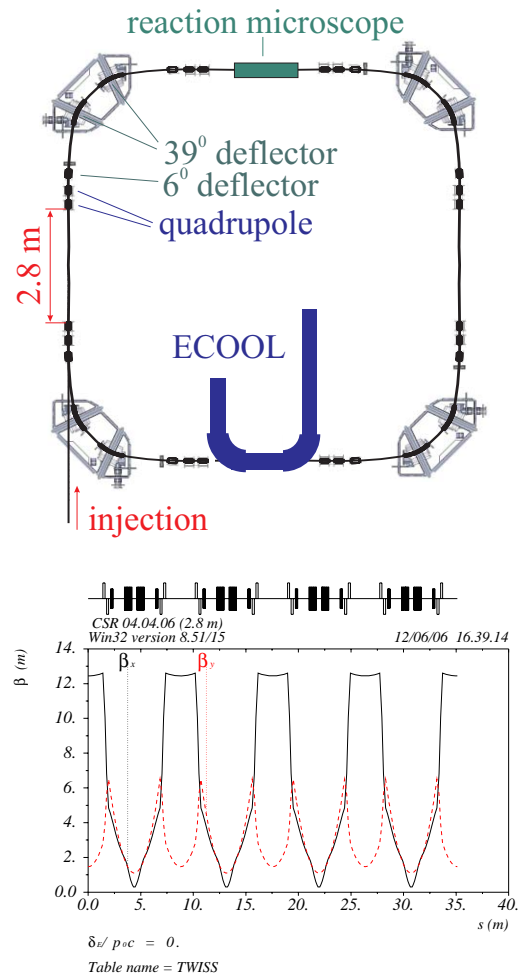


Figure 1: Up; layout of the CSR lattice, each cell consists of two 39°, two 6° deflectors and two quadrupole doublets. Down; horizontal ( $\beta_x$ ) and vertical ( $\beta_y$ ) betatron functions as calculated by the MAD code.

and after the corner sections are used. For the standard settings of the quadrupole strengths the horizontal and vertical  $\beta$ -functions of CSR are shown on the bottom of Figure 1. In the centre of the 2.8 m long straight sections the horizontal  $\beta$ -function reaches a maximum of 12.3 m, decreas-

\* Hicham.Fadil@mpi-hd.mpg.de

ing to a minimum between the two 39° deflectors. Related to the  $\beta$ -function are the tunes of the storage ring which are calculated to be horizontally  $\nu_x = 2.59$  and vertically  $\nu_y = 2.60$ . The dispersion of the storage ring reaches a maximum in the centre of the straight section of about 2.1 m.

### FINITE ELEMENTS CALCULATIONS

The CSR lattice described in the previous section was obtained with linear transfer matrices under the assumption that all elements are hard-edged. It is however clear that the actual optics elements will exhibit deviations from the ideal field distributions, as well as fringing fields. Hence, three dimensional numerical calculations of the realistic CSR elements were performed using the finite elements electrostatic code TOSCA. Exact geometrical models of the elements are created, and then the solution space is discretized with a 3 dimensional mesh. The fields, in particular the radial deflecting field  $E_r$ , are calculated for adequate boundary conditions, e.g. a grounded vacuum vessel, suitable potentials on the electrodes, and symmetry conditions where possible.

**The 39° and 6° Deflectors:** The main bending at the end of each section in the CSR will be done by two 39° cylindrical deflectors. This deflector is formed by 2 cylindrical electrodes 16 cm of height and gap of 6 cm. The radius of curvature is 1 m. Due to the finite dimensions of the deflectors, the nominal voltages are computed numerically. The calculated electric field distributions are shown in Figure 2. We observe (up) that the field distribution of the 39° deflector is very close to the ideal distribution of a cylindrical deflector. But the azimuthal electric field distribution along the ion orbit was found to have an important fringing field, which will affect the particle dynamics. We have therefore installed at each end of the deflector grounded electrodes at a distance of 15 mm, which serve as field clamps. The deflection angle of the 39° deflector was precisely calculated by tracking a single 300 keV proton, starting from the centre of the deflector and ending in a field free region. We find that the proton is deflected by about 40° and 41° with and without grounded electrodes respectively. This is due to the reduction of the fringing field. It is however of the utmost importance that the deflection angle of this element to be matched with the design value. We have therefore decided to trim (shorten) the deflector by 8.4 mm on each side, with which we could achieve our design value of the deflection angle of 39°. The 6° cylindrical deflector of the CSR consists of two cylindrical electrodes with a height of 24 cm and a gap of 12 cm. The ideal orbit has a curvature radius of 2 m. This deflector also utilises grounded electrodes to clamp the fringing field and is trimmed by 9.1 mm on each side in order to achieve a deflection angle of 6°. The radial field distribution as a function of the radial coordinate in the centre of the deflector deviates however by several percent from the

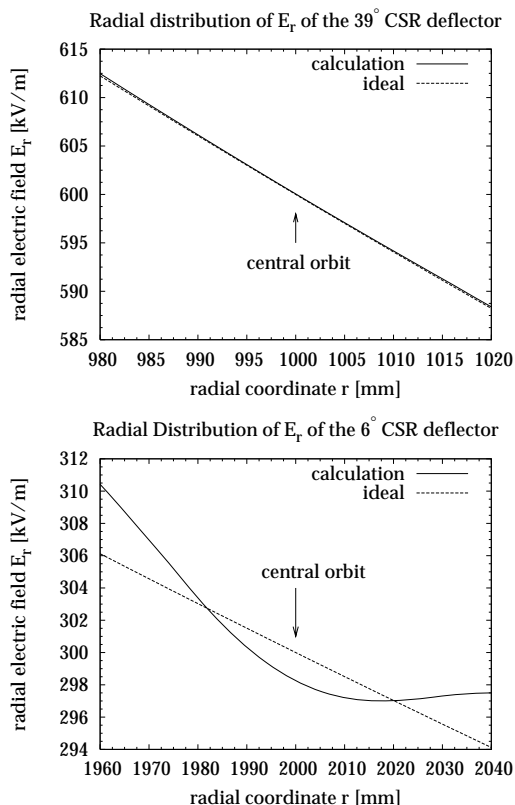


Figure 2: Up; calculated radial distribution of the electric field of the 39° cylindrical deflector is very close to the ideal case. Down; for the 6° deflector the deviation from the ideal field is large.

ideal field as shown on Figure 2 (down). This is mainly due to the limited azimuthal extent of the deflector and also to the rather large gap to height ratio (1:2).

**The Quadrupoles:** The transverse focusing in the CSR is done by two quadrupole doublets at the end of each straight section. For the CSR it was decided to use real hyperbolically shaped electrodes in order to achieve a quadrupole field as free from higher orders as possible. The inscribed radius of the quadrupole is 5 cm and the pole length is 20 cm. Due to the proximity of the two doublet quadrupoles, we have installed a grounded shield between them. Numerical calculations have shown that the two lenses of the doublet are effectively decoupled. The horizontal distribution of the deviations of the field gradient  $G(x) = dE(x)/dx$ , where  $E$  denotes the electric field, is shown on Figure 3(up). We observe that outside the region  $x = \pm 40$  mm there is a large deviation in the field gradient which will cause tune shifts and limit the ring acceptance. The longitudinal distribution of  $G_0(s)$  is shown on Figure 3 (down). We observe that the effective length of the quadrupole is about 6% larger than the electrode length of 20 cm. The quadrupole strengths will therefore be scaled down accordingly in order to achieve the same integrated field strength of the quadrupoles as the value used in the linear optics calculations.

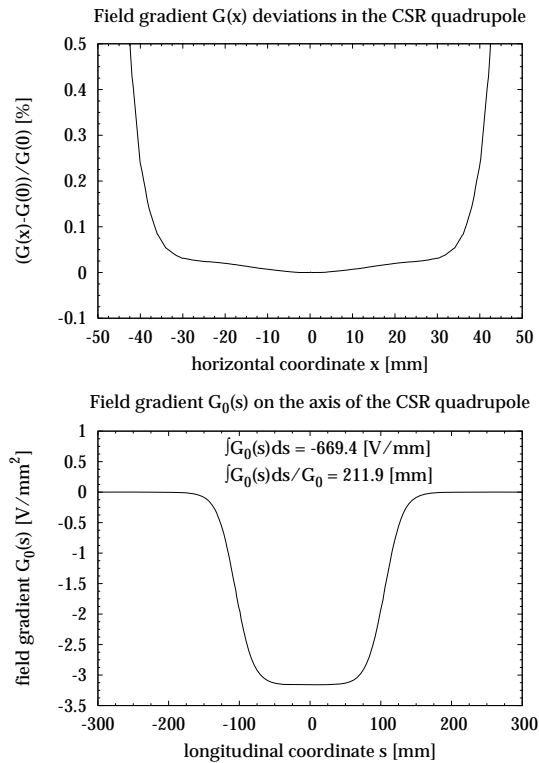


Figure 3: Up; horizontal dependence of the field gradient deviations in the CSR quadrupole. Down; the longitudinal dependence of the field gradient gives the effective length of 21.2 cm, which is about 6% larger than the electrode length of 20 cm.

**The Entire Ring:** After the calculation of the individual elements, a model of the entire ring was simulated in order to investigate the ion beam dynamics in the real fields of the CSR. In this model we have made use of all the symmetry conditions present in the CSR. After the field solution was obtained, tracking of a 300 keV proton was performed and we could store the particle for a maximum of 670 turns which was limited only by the program run time. In order to compare the lattice parameters with those found with the transfer matrix formalism, we have calculated the phase space ellipse of the stored particle at the centre of the straight section, then fitted the phase space ellipse equation to the data. The results are consistent as shown in Table 1. The dispersion at the centre of the straight section as well as the ring acceptance were also calculated, and the results are shown in Figure 4. The horizontal beam size of  $\pm 4$  cm is limited by the good field region in the quadrupoles. This means that we can fill our quadrupoles to about 80% (bore radius is 5 cm). The vertical acceptance is larger because of the smaller vertical beta function, and hence the smaller beam size inside the quadrupoles. In conclusion, we have shown that finite elements calculations of an entire accelerator structure is feasible and gives valuable insight on the performance of the machine.

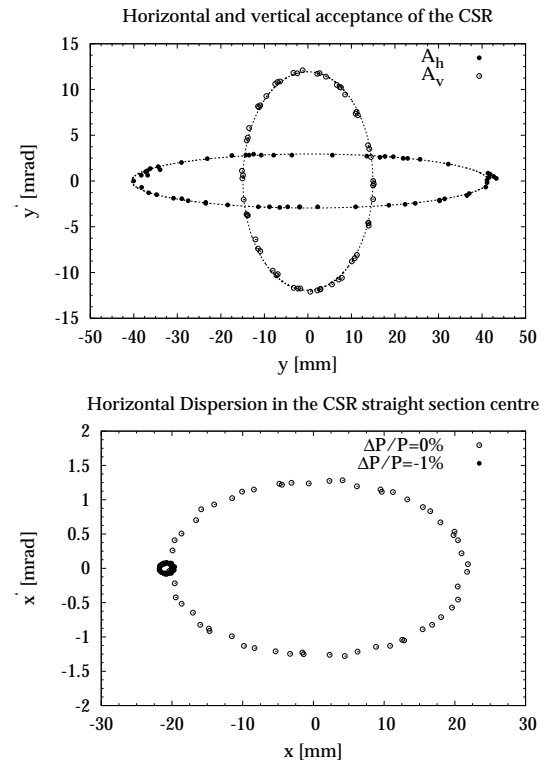


Figure 4: Up; the horizontal acceptance of the CSR is about 120 mm-mrad and the maximum horizontal beam size at the centre of the straight section is  $\pm 4$  cm. Vertically these figures are 180 mm-mrad and  $\pm 1.4$  cm respectively. Down; tracking an off-momentum particle ( $\Delta p/p = -1\%$ ) we find that the dispersion in the straight section is about  $D_x \approx 2.1$  m.

Table 1: Comparison of the main results from MAD and TOSCA.

Lattice	MAD	TOSCA
$\beta_x$ (m)	12.3	12.1
$\beta_y$ (m)	1.2	1.3
$D_x$ (m)	2.1	2.1
$\nu_x$	2.59	2.60
$\nu_y$	2.60	2.61
$A_x$ (mm-mrad)	—	120
$A_y$ (mm-mrad)	—	180

## REFERENCES

- [1] S.P. Møller, Nucl. Instrum. Methods in Physics Research A 394 (1997) 281.
- [2] T. Tanabe et al., Nucl. Instrum. Methods in Physics Research A 482 (2002) 595.
- [3] S. Jinno et al., Nucl. Instrum. Methods in Physics Research A 532 (2004) 477.
- [4] A. Wolf et al., Proc. COOL05 (2005) pp. 473-477.
- [5] D.A. Orlov et al., J. Physics: Conference Series 4 (2005) 290.